PROCEEDINGS OF SPIE

SPIEDigitalLibrary.org/conference-proceedings-of-spie

Integrated laser-induced fluorescence spectroscopy of donor-linker-acceptor constructs for bioenvironmental sensing

Sarah Mersch, Malachy Brink, Rowan Simonet, Arnold Boersma, Erin Sheets, et al.

Sarah A. Mersch, Malachy A. Brink, Rowan Simonet, Arnold J. Boersma, Erin D. Sheets, Ahmed A. Heikal, "Integrated laser-induced fluorescence spectroscopy of donor-linker-acceptor constructs for bioenvironmental sensing," Proc. SPIE 12228, Ultrafast Nonlinear Imaging and Spectroscopy X, 1222804 (3 October 2022); doi: 10.1117/12.2635951

SPIE.

Event: SPIE Optical Engineering + Applications, 2022, San Diego, California, United States

Integrated Laser-Induced Fluorescence Spectroscopy of Donor-Linker-Acceptor Constructs for Bioenvironmental Sensing

Sarah A. Mersch[a], Malachy J. Brink[a], Rowan Simonet[a], Arnold J. Boersma[b], Erin D. Sheets[a], Ahmed A. Heikal[a*]

[a]Department of Chemistry and Biochemistry, University of Minnesota, Duluth

[b]Cellular Protein Chemistry, Bijvoet Center for Biomolecular Research, Utrecht University

* aaheikal@d.umn.edu; Phone: 218-726-7036; Fax: 218-726-7394.

Keywords: FRET, biosensors, time-resolved anisotropy, time-resolved fluorescence, FCS-FRET, macromolecular crowding, intracellular ionic strength, and donor-linker-acceptor.

ABSTRACT

The heterogeneous cellular environment influences a myriad of biological processes. For example, macromolecular crowding affects biochemical reactions, protein-protein interactions, and protein folding. Additionally, the structure-function relationship of biomolecules and enzymatic activities are sensitive to the surrounding ionic strength. In this contribution, we highlight our recent studies on a family of donor–linker–acceptor constructs, which were designed for mapping the macromolecular crowding and ionic strength in living cells. Integrated ultrafast laser spectroscopy methods have been employed to quantify the Förster resonance energy transfer (FRET) and the donor-acceptor distance as a measure of the sensitivity of these constructs to environmental changes. The donor-acceptor FRET pairs are intrinsically fluorescent cyan and yellow proteins, respectively, that can be genetically encoded in living cells. The sensitivity of these constructs to environmental biomimetic crowding and ionic strength was investigated as a function of the sequence and charge of the linker regions, as well as the identity of the donor protein. Integrating non-invasive, quantitative laser-induced fluorescence methods with FRET, as a molecular ruler, provides a powerful tool for cellular studies towards mapping out macromolecular crowding and ionic strength in living cells. Our results are key for the development of rational design strategies for engineering enhanced noninvasive biosensors with better environmental sensitivities. The same sensors were used as a model system for developing new experimental approaches for protein-protein interaction and FRET studies. Importantly, these diagnostic molecular and analytical tools set the stage for understanding the correlation between these environmental factors and cellular functions.

1. INTRODUCTION

The heterogenous cellular environment (e.g., macromolecular crowding, ionic strength, etc.) influences a myriad of biological processes, but our understanding of these dynamic environments is limited by the site-specificity of environmental sensors or labels, the spatial and temporal resolutions of employed methodologies, and the biological limitations of model systems.[1–4] Macromolecular crowding, for example, influences biochemical reactions, protein-protein interactions, and protein folding.[5–11] It is estimated that macromolecular crowding in cells varies within an estimated range of 80-300 g/L across cytoplasm and organelles.[9,12–14] Additionally, the structure-function relationship of biomolecules, enzymatic activities, and cellular osmolarity are sensitive to the compartmentalized intracellular ionic strength.[15,16]

Macromolecular crowding also been tied to changes in osmotic pressure and diffusion rates of biomolecules.[17] Both crowding and osmotic pressure are frequently investigated by compressible probes, such as labelled polymers[18,19] or intrinsically disordered proteins.[20,21] Diffusion coefficients can be measured using

Ultrafast Nonlinear Imaging and Spectroscopy X, edited by Zhiwen Liu, Demetri Psaltis, Kebin Shi, Proc. of SPIE Vol. 12228, 1222804
 · 0277-786X · doi: 10.1117/12.2635951

a large array of techniques, such as fluorescence correlation spectroscopy (FCS),[22,23,23–25] fluorescence recovery after photobleaching,[22] and single-particle tracking,[26] which rely on the diffusion of a fluorescent particle across a defined observation volume and the corresponding diffusion time is then related to the diffusion coefficients within the context of the environmental crowding. These fluorophores encompass intrinsically fluorescent proteins[26,27], functionalized nanoparticles[28], quantum dots[26,29,30], or fluorescent dyes.[26,27,31] Direct measurements of bulk ionic strength are less common; instead, most researchers focus instead on detection of individual ions of interest. Usually, individual ion sensing measurements take advantage of ion binding domains (or chemosensors) for quantification.[32–35] Recently, Altamash *et al.* has published a bioluminescence-based approach for probing bulk ionic strength.[36] It was determined that the bioluminescence of NanoLuc reversibly decreases in response to NaCl and KCl addition and a BRET-based biosensor was created from fusing NanoLuc to mNeonGreen.[36]

Förster resonance energy transfer (FRET), considered a molecular ruler, is a quantitative method for observing protein-protein interactions, intermolecular interactions, and conformational changes of biomolecules.[1,37] FRET is a non-radiative, dipole-dipole interaction where energy from an excited donor molecule is transferred to an acceptor molecule in close proximity (1-10 nm).[38–41] The FRET efficiency depends on the donor-acceptor distance, the relative orientation of the donor emission and acceptor absorption dipoles, and the spectral overlap between donor emission and acceptor absorption.[38,40,41] A number of methods exist to quantify FRET, such as steady-state fluorescence spectroscopy,[42,43] time-resolved fluorescence,[1,4,42,43] and single molecule fluorescence.[44,45]

In this minireview, we highlight recent developments of environmental sensors that consist of donor-linker-acceptor constructs with variable amino acid sequences, lengths, flexibility, and charge of the linker region. The donor molecule (mCerulean3) is a cyan fluorescence protein (CFP), and the acceptor molecule (mCitrine) is a yellow fluorescent protein (YFP). This donor-acceptor FRET pair is photostable with a high quantum yield and, importantly, without the tendency to form aggregates.[46–48] The sensitivity of these sensors to the surrounding environment, either macromolecular crowding or ionic strength, are characterized using complementary laser spectroscopy techniques for FRET analysis and the donor-acceptor distances. These studies aim at the development of rational design strategies for FRET-based environmental sensing, both in controlled environments and ultimately for use in *in vivo* environments. In addition, we examine the correlation between the newly developed fluorescence approaches (time-resolved fluorescence depolarization and single molecule fluorescence fluctuation) for FRET analysis as compared with the traditional time-resolved and steady state fluorescence spectroscopy methods on the same molecular systems.

2. MACROMOLECULAR CROWDING SENSORS

2.1 Engineering of Genetically Encoded Donor-Linker-Acceptor Constructs for Site-Specific Crowding

Boersma *et al*. developed a FRET-based fluorescent biosensor, GE, as a macromolecular crowding probe in the form of an mCerulean3-linker-mCitrine construct.[46] This sensor used a hinge-like linker design that connected the donor cyan fluorescent protein, mCerulean3, with the acceptor yellow fluorescent protein, mCitrine, by two α-helices and random coils. Following a similar design strategy, Boersma and coworkers have since developed a family of variants with different amino acid sequences in the linker region to examine the effects of the length and flexibility of the linker region on the environmental sensitivity (Table 1). The family of these new constructs consists of nine macromolecular crowding variants (E6G2, E6G6, E4G2, E4G6, E6, G12, G18, and G24) where the number and length of the α-helices and inner $(GSG)_n$ in the linker region were varied (Figure 1).[47,49]

Table 1: Amino acid sequence of the linker region of selected mCerulean3-linker-mCitrine constructs used as macromolecular crowding sensors.

Crowding Sensor	Amino Acid Sequence of the Linker Region
GE	– $(GSG)_6A(EAAAK)_6A(GSG)_6A(EAAAK)_6A(GSG)_6$–
E6G2	–$A(EAAAK)_6A(GSG)_2A(EAAAK)_6A$–
E6	– $(GSG)_6A(EAAAK)_6A(GSG)_6$–
G12	– $(GSG)_{12}$–
G18	– $(GSG)_{18}$–

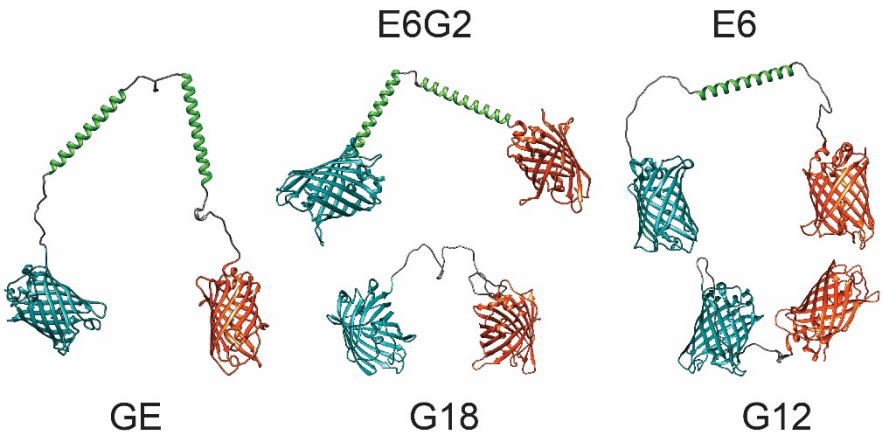

Figure 1: Schematic representation of selected donor-linker-acceptor constructs designed for macromolecular crowding sensing.[50,51]

We hypothesize that as macromolecular crowding increases, the surrounding steric hinderance leads to a collapsed conformation of these donor-linker-acceptor constructs, which in turn decreases the donor-acceptor distance and, therefore, increases the FRET efficiency (Figure 2). Hus, the constructs can be considered as a tool to measure of sensitivity to environmental crowding, was measured *in vivo* using two-channel confocal microscopy studies on *E. coli* strain BL21(DE3)pLysS and *in vitro* using steady-state fluorescence spectroscopy of samples in a cuvette. It was demonstrated that the sensors without α-helices (G12, G18, G24) showed the highest FRET efficiency, which was attributed to higher linker flexibility and shorter linker distance.[49] All sensors responded to increasing amounts of Ficoll-70 (70 kDa), up to 40% (w/w), recorded as an increase in relative mCitrine/mCerulean3 fluorescence intensity, which was attributed to FRET. The larger probes (E6G2, GE) had a larger overall compression in Ficoll-70, up to 85%, which was attributed to the increased size and stiffness of the linker and therefore an increased donor and acceptor distance in an uncrowded environment. Additionally, it was also determined that the changing FRET efficiency of these probes was due to crowding alone, because the probes were sensitive to a variety of crowding agents (polyethylene glycol [PEG], ubiquitin, BSA) but did not respond to salts or common metabolites.[46,49]

Importantly, *in vivo* expression and corresponding steady-state spectroscopy of these probes in *E. coli* suggested that α-helices were necessary for compression of the probes in cells. The observed effect was likely more dependent on the (EAAAK)/(GSG) ratio than on linker length,[49,54] which was attributed to of the reduced flexibility of the linkers with higher (EAAAK)/(GSG) ratios.[54] However, it was concluded that future

molecular engineering design must optimize the balance among the linker rigidity, length, and flexibility towards an enhanced sensitivity of donor-linker-acceptor sensors to macromolecular crowding.[49,54]

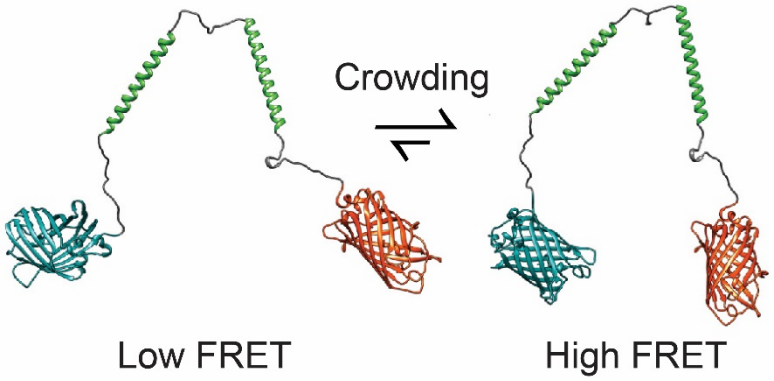

Figure 2: Hypothesized mechanism that underlies the response of mCerulean3-linker-mCitrine constructs to surrounding environmental crowding. At high concentration of macromolecular crowding, the FRET efficiency increases due to steric hindrance that favors the collapsed conformation.[49–53]

Steady state intensity FRET has many advantages, including easy availability, low cost, ease of operation, and minimum photon waste.[42] However, the steady-state approach may suffer from complications due to spectral overlap (bleed-through or cross-talk) between the detection channels of the donor and acceptor, different detection efficiencies, and the potential of exciting the acceptor directly.[43] Valuable samples (cells, tissues, or proteins) are also not well-suited for cuvette-based steady-state spectroscopy.[42] Additionally, protein sensors must be expressed a relatively high concentrations to generate a reasonable signal-to-noise ratio while suppressing the intrinsic cellular autofluorescence of native biomolecules that may interfere with FRET analysis. For cellular crowding studies, cells transfected with the donor-linker-acceptor construct must be compared with cells expressing the donor alone as a control. It is also believed that the steady-state spectroscopy approach may lead to averaging over multiple molecular conformations (or states) as well as an overestimated donor-acceptor distance.

2.2 Crowding Sensitivity of Donor-Linker-Acceptor Constructs using Time-Resolved Fluorescence of the Donor

To overcome the challenges associated with a steady-state spectroscopy approach, time-resolved fluorescence measurements (Figure 3) were reported on the family of crowding sensors[50,52] shown in Figure 1. The fluorescence lifetime of a fluorophore is sensitive to aspects of its chemical structure as well as its surrounding environment, but, unlike a steady-state spectroscopy approach, the fluorescence lifetime is not sensitive to the fluorophore concentration.[1,40] In addition, time-resolved fluorescence measurements of a FRET pair are capable of differentiating between subpopulations undergoing FRET at different rates. Finally, time-resolved fluorescence is the main observable in fluorescence lifetime imaging microscopy (FLIM), which is compatible with live cells and tissue imaging at high spatial and temporal resolutions.[1,4] With careful experimental design and data analysis, fluorescence lifetime measurements of FRET pairs in living cells may rule out the need for transfecting the cells with the donor alone as a control.

The excited-state fluorescence lifetime of the donor in these constructs was measured for cleaved (no FRET) and intact (FRET) sensors as a function of the surrounding environmental crowding. In an ensemble of donor-linker-acceptor constructs, it was assumed that not all sensors will undergo FRET coherently and there are likely two subpopulations, one that undergoes FRET and another that does not. With these assumptions in mind, the observed fluorescence decays, $F(t)$, of the donor in intact sensors were modeled as a biexponential, such that:[50,52,55]

$$F(t) = \alpha_1 e^{-(k_{ET}+k_f^D)t} + \alpha_2 e^{-(k_f^D)t} \quad (1)$$

In this model, the first term represents the subpopulation that undergoes FRET (at an amplitude fraction α_1) where the fluorescence decays at a sum of rates ($k_{ET} + k_f^D$) of the involved processes. The second term represents the fluorescence decay of the donor at a rate of k_f^D without FRET (at an amplitude fraction α_2).

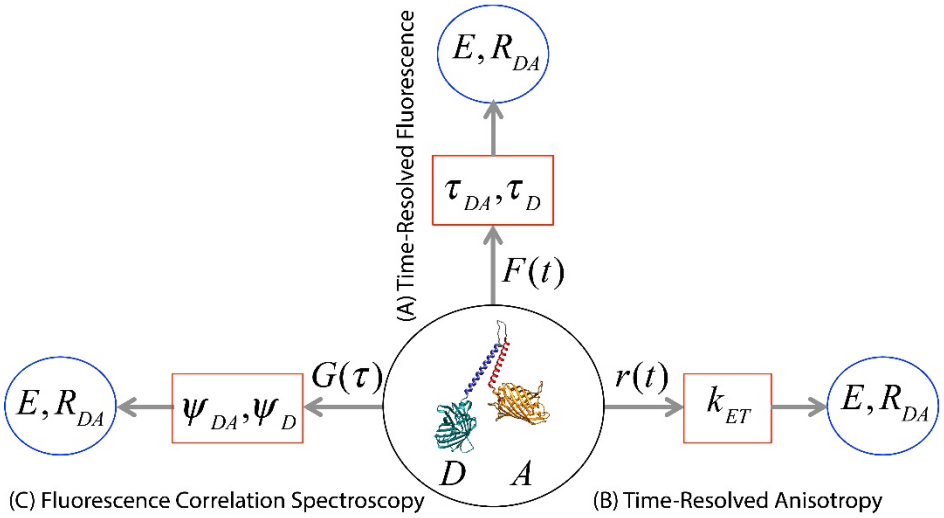

Figure 3: A sketch of integrated fluorescence approaches for FRET analysis of donor–linker–acceptor constructs for environmental sensing. (A) Time-resolved fluorescence of the donor in the presence and absence of the acceptor. (B) Time-resolved fluorescence depolarization (anisotropy), where the donor is excited, and the dominant emission of the acceptor is polarization analyzed. (C) Fluorescence correlation spectroscopy (FCS) for measuring the molecular brightness of the donor in the presence and absence of the acceptor at the single molecule level.

In these measurements, the fluorescence was detected at magic-angle polarization[40,56] to rule out the effects of rotational dynamics during the excited state lifetime. In the absence of FRET, the time-resolved fluorescence decays as a single exponential with a fluorescence decay (k_f^D) close to the inverse of the fluorescence lifetime (τ_D) of the donor alone. From Equation (1) the energy transfer efficiency (*E*%) can be calculated using the fluorescence lifetime of the donor in the presence (τ_{AD}) and absence (τ_D) of the acceptor such that:[50,52,55]

$$E_1(\%) = \left(1 - \frac{\tau_{DA}}{\tau_D}\right) \times 100 \quad (2)$$

Using this approach, Currie *et al.*[52] compared the time-resolved fluorescence lifetime of cleaved (no FRET) and intact (FRET) GE for FRET analysis. In the absence of FRET, the cleaved GE fluorescence decayed as a single exponential as compared with the biexponential in the presence of energy transfer from the donor to the acceptor (Equation 1) in the intact sensor, where the FRET efficiency and donor-acceptor distance were reported.[52] Under the 465-nm excitation of cleaved and intact GE, the time-resolved fluorescence (detected the acceptor at 530/40-nm) decayed as a single exponential in the absence of FRET. Under the same experimental conditions, the authors also carried out control experiments on free cyan

fluorescent protein and free yellow fluorescent protein to examine the effects of mCerulean3 and mCitrine mutations in GE sensor.

Schwartz *et al*.[50] have reported comprehensive time-resolved fluorescence studies of the donor in several of the aforementioned molecular crowding sensors (GE, G12, G18, E6G2, and E6), which agreed with the steady-state results presented by Boersma *et al*. Under 425nm pulsed excitation of the donor, the fluorescence decay of the donor in the presence (intact, FRET) and absence (cleaved, no FRET) of the acceptor were used to calculate the corresponding FRET efficiency and the donor-acceptor distance as a function of the Ficoll-70 concentrations. As the Ficoll-70 concentration increased, the energy transfer efficiency increased, and the corresponding donor-acceptor distance decreased due to enhanced crowding-induced steric hindrance.[50] This study also showed that crowding sensors without α-helices had the highest FRET efficiency. Sensors with α-helices in the linker region, however, showed a larger dynamic range in their response to increasing concentrations of the crowding agent.

The results support the hypothesis that steric hinderance at higher Ficoll-70 concentrations increases the FRET efficiency (i.e., smaller donor-acceptor distance) and therefore results in higher sensitivity to environmental crowding.[50] To differentiate between crowding and homogeneous viscosity effects on the observed FRET efficiency, Schwartz *et al*. repeated the same measurements of the same family of crowding sensors, both cleaved and intact, as a function of glycerol concentrations. It was demonstrated that the higher homogeneous viscosity stabilized the stretched conformation and a decrease in thermal fluctuations, which resulted in either no change or a reduction in the FRET efficiency. The detailed amino acid sequence of the linker region between the donor and acceptor in those sensors was invoked in data interpretation. For example, the sensitivity of sensors with random coil linker (G12 and G18) exhibited the largest response to changing viscosity and the dual α-helix linkers (GE and E6G2) remained essentially unchanged.[50]

2.3 Using Crowding Sensors for Technique Development

2.3.1 Time-resolved fluorescence depolarization for FRET analysis

Traditionally, time-resolved fluorescence anisotropy is used for studying the rotational dynamics and conformational mobility of fluorophores during their excited-state lifetime.[40] In time-resolved anisotropy measurements, the time resolved parallel $I_{//}(t)$ and perpendicular $I_{\perp}(t)$ fluorescence polarizations are detected and used to calculate the corresponding anisotropy decay, $r(t)$, for a given molecule, such that:[40]

$$r(t) = \frac{I_{//}(t) - I_{\perp}(t)}{I_{//}(t) + 2I_{\perp}(t)} \tag{3}$$

For a simple molecule rotating in an environment with a homogenous viscosity, the anisotropy decay can be modeled as a single exponential with a rotational time (φ_r) and an initial anisotropy (r_0) where:[40]

$$r(t) = r_0 \cdot e^{-t/\varphi_r} \tag{4}$$

The initial anisotropy (r_0) is related to the angle between the absorbing and emitting dipole of the excited molecule during the excited state lifetime. According to the Stokes-Einstein model, the rotational time (φ_r) depends on the hydrodynamic volume (V) and the viscosity (η) of the surrounding environment at a given temperature (T), where k_B is Boltzmann's constant, such that:[40]

$$\varphi_r = \frac{\eta V}{k_B T} \tag{5}$$

Recently, Heikal and coworkers proposed the use of a similar approach to time-resolved anisotropy for investigating the fluorescence depolarization of donor-linker-acceptor constructs due to both hetero-FRET and rotational dynamics (Figure 3).[51,52,57] Upon pulsed excitation of the donor, the time-resolved fluorescence of mostly the acceptors emission is analyzed into parallel and perpendicular polarizations of the donor-linker-acceptor construct in a given environment. In an ensemble of donor-linker-acceptor constructs, it is assumed that a fraction of the population, $f_1(\lambda)$, will undergo depolarization (or anisotropy) due to FRET (fast) and another fraction, $f_2(\lambda)$, will only undergo rotation (slow) such that the overall time-resolved anisotropy can be modeled as:

$$r(t) = f_1(\lambda) \cdot r_1(t) + f_2(\lambda) \cdot r_2(t) \tag{6}$$

In this proposed model, the first term represents a subpopulation that undergoes depolarization $r_1(t)$ due to FRET when the detected emission is dominated by the acceptor's emission $f_1(\lambda)$. The second term, however, represents the depolarization $r_2(t)$ of a subpopulation due to rotational mobility alone, which dominates when the donor's emission $f_2(\lambda)$ is detected. The time-resolved ensemble anisotropy $r(t)$ of hetero-FRET pairs can be written as:

$$r(t) = f_1(\lambda) \cdot \beta_1 e^{-(k_{ET} + \varphi_r^{-1}) \cdot t} + f_2(\lambda) \cdot \beta_2 e^{-(\varphi_r^{-1}) \cdot t} \tag{7}$$

The sum $\beta_1 + \beta_2$ in this model equals the initial anisotropy (r_0). The contributions of each subpopulation to the overall fluorescence depolarization $f_1(\lambda)$ and $f_2(\lambda)$ depend on the fluorescence quantum yield of the donor and acceptor as well as their peak emissions, which can be adjusted using different emission filters. For example, when exciting and detecting exclusively the donor emission of a hetero-FRET pair, the second term due to rotation-induced depolarization will dominate. When exciting the donor and detecting mainly the acceptor emission, the first term due to FRET will dominate. The observed time-resolved anisotropy can be used to calculate the energy transfer rate (k_{ET}) and therefore the energy transfer efficiency (E%) using the following equation:[40,57]

$$E_2(\%) = \left(\frac{k_{ET}}{k_{ET} + \tau_D^{-1}} \right) \times 100 \tag{8}$$

It is worth emphasizing that monitoring the rotational dynamics is limited by the excited state fluorescence lifetime of the donor (τ_D).

Currie *et al*. demonstrated this time-resolved fluorescence depolarization approach for FRET analysis using intact and enzymatically cleaved GE sensor (mCerulean3-linker-mCitrine) as a model system.[52] First, the time-resolved anisotropy of the donor's emission (425-nm excitation and 475/50-nm polarized detection) in both the cleaved (no FRET) and intact (FRET) decayed as a single exponential. As expected, the anisotropy of cleaved GE decayed with a faster rotational time than the intact counterpart due to the difference in hydrodynamic volumes. However, the estimated overall rotational time of the intact GE was slightly faster than the theoretical predictions based on sensor molecular weight, which was attributed to

potential segmental mobility due to the flexible linker.[52] Under these conditions, the fluorescence depolarization of the donor in the presence or absence of the acceptor was attributed mainly to the corresponding rotational mobility (i.e., no FRET). Second, the time-resolved fluorescence depolarization of intact GE, using 425-nm excitation of the donor and 531/30 nm polarized detection of mostly the acceptor, decayed as a biexponential where the faster decay component was attributed to FRET[52] while the slow decay component was due to the overall rotational dynamics (Equation 7). The time-resolved fluorescence depolarization of the cleaved GE sample, however, decayed as a single exponential due to rotational dynamics alone.

Leopold *et al*. reported comprehensive studies of a family of crowding sensors (GE, G12, G18, E6G2, and E6) using time-resolved fluorescence depolarization as a function of macromolecular crowding using Ficoll-70 as a crowding agent.[51] The objective of these studies was to examine the sensitivity of the time-resolved anisotropy approach to the linker design in these sensors under 425-nm pulsed excitation and 531/30-nm polarized detection. Using E6, Leopold and colleagues demonstrated that the FRET-incapable cleaved sample produced a single exponential decay, while a FRET-capable sensor required biexponential fitting. Again, the fast component of the biexponential decay was attributed to FRET.

Importantly, while GE, E6, and E6G2 decayed satisfactorily as a biexponential, the anisotropy decays of G12 and G18 were better described by a triple exponential that was attributed to different rates of FRET between two distinct FRETing populations in these samples. Overall, both increased length and stiffness of the linker region were correlated to a decrease in FRET; however, length is thought to be the predominating factor influencing FRET.[51] Leopold *et al*. also observed decreasing FRET as a function of glycerol and an increase in the slow rotating fraction of the population. This observation was also attributed to the stabilization of the stretched conformation in a more viscous environment.

2.3.2 Fluorescence correlation spectroscopy and molecular brightness FRET analysis at the single molecule level

Time-resolved fluorescence and anisotropy on molecular ensembles have the potential of washing out interesting single molecule states or processes due to the inherent averaging over a large number of molecules. In contrast, single molecule studies using a wide range of techniques provide a means to avoid such ensemble averaging limitation.[58,59] One of these single molecule techniques is fluorescence correlation spectroscopy (FCS) in all its modalities.[25,60,61] In the simplest modality of FCS experiments, for example, an open observation volume ($\sim 1 \times 10^{-15}$ L) is created using both the laser excitation and the confocal epifluorescence. As molecules at nanomolar concentrations diffuse freely in and out of the observation volume the time-dependent fluorescence fluctuation is detected using single-molecule detectors (e.g., avalanche photodiodes, APDs). This fluorescence fluctuation is autocorrelated with itself to create the corresponding autocorrelation curve, which yields the average number of molecules residing in the observation volume, the translational diffusion time, and any other processes beside diffusion that contribute to such fluctuations (e.g., fluorescence blinking in intrinsically fluorescent proteins, binding kinetics, and triplet state population via intersystem crossing).[25,60–62]

There have been more sophisticated modalities of FCS used for FRET analysis, which include fluorescence cross-correlation spectroscopy, FCCS,[63,64] and dual-color FCCS.[65,66] In the FCCS approach, the fluorescence fluctuations of both the donor and acceptor are detected using different APDs simultaneously and the corresponding cross-correlation curve of the donor-acceptor pair is calculated. For FRET analysis, however, the molecular brightness, the quantum yield, spectral overlap, and the detection efficiency of both the donor and acceptor must be accounted for, which is not trivial. In addition, the details of the fitting model used for the cross-correlation curve analysis also matters.

Recently, Kay *et al*. proposed a much simpler approach using the traditional FCS modality using a continuous wave (cw) laser for FRET analysis of donor-linker-acceptor constructs (Figure 3).[53] It is known that the traditional steady-state, time-averaged fluorescence intensity of the donor in the absence (F_D) and presence (F_{DA}) of the acceptor can be used to calculate the corresponding energy transfer efficiency (E%) such that:[53]

$$E_3(\%) = \left(1 - \frac{F_{DA}}{F_D}\right) \times 100 \tag{9}$$

In their approach, Kay *et al*. used FCS to measure the time-averaged fluorescence fluctuation, $\langle \delta F_i(t) \rangle$, and the number of molecules, N, (e.g., either intact or cleaved donor-linker-acceptor constructs) that are residing in a calibrated observation volume. In traditional FCS, the measured time-dependent fluorescence fluctuation at a given time can be autocorrelated with itself as a function of lag time (τ) to obtain the fluorescence fluctuation autocorrelation function $G(\tau)$ such that:[25,60,61]

$$G(\tau) = \frac{\langle \delta F(t) \otimes \delta F(t+\tau) \rangle}{\langle \delta F(t) \rangle^2} \tag{10}$$

For fluorescence fluctuations due to translational diffusion alone (i.e., no chemical kinetics, triplet state intersystem crossing, or fluorescence blinking), the autocorrelation function $G(\tau)$ for a molecule depends on the number of molecules (N), the diffusion time (τ_d), and the axial-to-lateral dimensions ($\omega = r_z / r_{xy}$) of the observation volume such that:[25,60,61]

$$G(\tau) = \frac{1}{N} \frac{1}{\left(1 + \tau / \tau_d\right)} \frac{1}{\sqrt{\left(1 + \tau / \omega^2 \tau_d\right)}} \tag{11}$$

With the measured number of molecules (N_i) and the time-averaged fluorescence fluctuations (δF_i), the corresponding molecular brightness, ψ_i, (i.e., the number of detected fluorescence photons per molecule in the observation volume) was then calculated for both the cleaved ($i = D$) and intact ($i = DA$) constructs under the same experimental conditions using the following equation:[53]

$$\psi_i = \frac{F_i(t)}{N_i} = \frac{\langle \delta F_i(t) \rangle}{N_i} \tag{12}$$

The estimated molecular brightness, instead of the time-averaged fluorescence intensity, rules out any differences in the concentrations of the prepared sample of cleaved and intact FRET constructs used as environmental sensors. As a result, Equation (9) can be rewritten in terms of the molecular brightness to estimate the energy transfer efficiency at the single molecule level, where:[53]

$$E_4(\%) = \left(1 - \frac{\psi_{DA}}{\psi_D}\right) \times 100 \tag{13}$$

This simple approach requires only a single detector for the traditional FCS experiments, where the donor's emission is excited and detected in the presence and absence of the acceptor for FRET analysis. Additionally, spectral overlap can be ruled out by careful selection of the emission filter for the donor alone. Unlike dual-color FCCS, the proposed traditional FCS approach does not require two excitation lasers for exciting the donor and acceptor simultaneously and therefore rules out the need for exact knowledge of either the detection efficiency of the donor or the fitting model of the autocorrelation curve.

Kay *et al*. demonstrated the FCS-FRET approach on two variants of donor-linker-acceptor constructs for macromolecular crowding sensing (namely, GE2.1[47] and GE; GE2.1 uses mTurquoise2.1 as a donor) as a proof-of-concept.[53] The donor in each sensor was excited at 405-nm and the fluorescence fluctuation of cleaved and intact sensor was detected at 475/50 nm. They hypothesized that the molecular brightness of the donor molecule alone (i.e., in the absence of FRET) would be higher than the donor in the presence of an acceptor (i.e., in the presence of FRET). They determined that, despite a smaller number of molecules in the observation volume, the donor alone samples of both GE2.1 and GE had larger fluorescence fluctuations and therefore higher molecular brightness than intact donor-acceptor constructs which was attributed to the presence of FRET in the intact constructs. Importantly, the increased molecular brightness of the donor in the presence and absence of the acceptor (and therefore FRET efficiency) was not sensitive to the laser intensity within the linear region. At the single-molecule level, the reported FCS-FRET efficiencies of both sensors were slightly higher than those determined using the ensemble averaged time-resolved fluorescence lifetime.[50,52]

As a control, Kay *et al.* directly excited the acceptor molecule using a 488-nm laser (continuous wave) to verify the hypothesis that the intact donor-acceptor construct and the donor alone would have the same brightness due to the absence of FRET.[53] While the intact GE2.1 construct did have a slight increase in brightness relative to the mTurquoise2.1 donor alone, this characteristic was thought to be the result of enhanced spectral overlap in this sensor, and the GE construct displayed similar molecular brightness for both the intact construct and the donor alone. The increased brightness of the donor alone under 405-nm excitation and the minimal difference between donor alone and the intact constructs under 488-nm excitation demonstrates the potential of using the traditional FCS for FRET analysis of donor-linker-acceptor constructs.

3. IONIC STRENGTH SENSORS

3.1 Engineering of Genetically Encoded Donor-Linker-Acceptor Constructs for Environmental Ionic Strength Sensing

Boersma and coworkers have also developed a family of ionic strength sensors (RD, RE, and KE), which consists of donor-linker-acceptor constructs (Table 2) with two oppositely charged α-helices in the linker region.[67] The oppositely charged α-helices in the linker region were created by the insertion of glutamate/aspartate and lysine/arginine residues into the amino acid sequence of the two α-helices in those constructs. These probes were found to be sensitive to the ionic strength of their environment, with some dependency on the anion identity.[67] The ionic strength sensitivity of those sensors correlated to the Hofmeister series of salts in terms of the hydration level of common anions. These ionic strength sensors also exhibit some sensitivity to other environmental factors such as macromolecular crowding, pH, and the temperature.

These genetically encoded ionic strength sensors were expressed in HEK293 cells and their environmental sensitivity (i.e., FRET efficiency) was monitored by steady-state spectroscopy *in vitro* (96-well plate in a Spark microplate reader) and *in vivo* (two-channel confocal microscopy). In those steady-state studies, the emission peak ratio of the mCitrine/mCerulean3 within cells was quantified as an indication of

the FRET efficiency (i.e., sensitivity) as a function of the cell titration the ionophores valinomycin and nigericin.[67]

Table 2: Amino acid sequence of the linker region of mCerulean3-linker-mCitrine constructs (RE, RD, and KE) used as ionic strength sensors.

Ionic Strength Sensor	Amino Acid Sequence of the Linker Region
RE	–A(AAAAR)$_6$A(GSG)$_6$A(EAAAA)$_6$A–
RD	–A(AAAAR)$_6$A(GSG)$_6$A(DAAAA)$_6$A–
KE	–A(AAAAK)$_6$A(GSG)$_6$A(EAAAA)$_6$A–

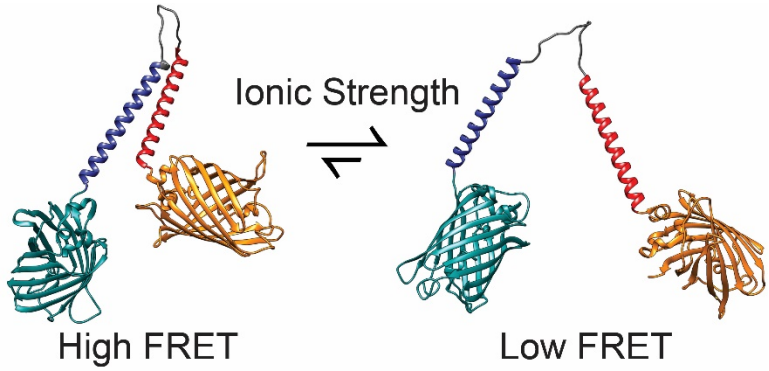

Figure 4: Hypothesized mechanism for the response of these donor-linker-acceptor constructs to surrounding environmental ionic strength. As the ionic strength increases, the FRET efficiency decreases due to Debye ionic shield that reduces the electrostatic interactions between the charged α-helices in the linker region.[52,55,57,67]

3.2 Quantifying the Sensitivity of Ionic Strength Sensors (i.e., FRET Efficiency) in Controlled Solutions using Time-Resolved Fluorescence Measurements

Steady state spectroscopy studies for FRET analysis are prone a few issues such as spectral overlap, ensemble averaging, and concentration dependence of the steady state fluorescence signal, which can be overcome using time-resolved fluorescence measurements. As a result, Miller *et al*. used time-resolved fluorescence of the excited electronic state of the donor, in the presence and absence of the acceptor, of the same family of the mCerulean3-linker-mCitrine constructs (Table 2, Figure 3) for ionic strength sensing.[55,67]

Under 425-nm pulsed laser excitation of the donor, the time resolved fluorescence of the donor (475/50-nm and magic-angle detection) was measured in the presence and absence of the acceptor of RD, RE, and KE sensors in buffer. Using the fitting parameters of those fluorescence decays as discussed above, the energy transfer efficiency was determined for those sensors along with the donor-acceptor distance to identify the most sensitive sensor in this family based on the amino acid sequence of the linker region. It was reported that the time-resolved fluorescence of the intact sensors was best fit as biexponential decay as compared with the single exponential decay for the cleaved counterpart. The fast decay component of those biexponential decays of the intact sensors was attributed to FRET in the presence of the acceptor. The slow decay component was attributed to a subpopulation of the intact sensors without FRET due to perhaps the unfavorable dipole orientations of the donor-acceptor pairs or thermally stretched linker region.

Miller *et al*. also hypothesized that as the ionic strength increases, the dissolved ions will reduce the electrostatic interaction (Debye ionic shielding, Figure 4) between the two oppositely charged α-helices in the linker region and therefore will increase the donor-acceptor distance, thereby leading to a reduction of the FRET efficiency in a manner that is sensitive to the type of dissolved ions.[55] To test this hypothesis, Miller *et al*. used time-resolved fluorescence of the donor of the ionic-strength sensors (RD, RE, and KE) in the presence and absence of the acceptor as a function of the ionic strength using different Hofmeister salts (KCl, LiCl, NaCl, NaBr, NaI, Na_2SO_4).[55] In addition, controlled studies on similar donor-linker-acceptor constructs with a neutral linker region were carried out as a control under the same experimental conditions. The sensors KE, RE, and RE showed the largest response to NaI, demonstrating a sensitivity to the extreme end of the Hofmeister series.[55] They reported that the energy transfer efficiency of RD, RE, and KE sensors deceased as the ionic strength of potassium chloride (KCl) solution increased, which supported their hypothesis. In addition, the donor-acceptor distance in these constructs increased with the ionic strength in KCl solutions. The energy transfer efficiency also showed a minor dependence on the linker sequence. As a control, KCl concentration (pH 7.4) had no significant effect on the FRET efficiency or the donor-acceptor distance of E6G2 probe with a neutral α-helix under the same experimental conditions.[55]

3.3 Testing the Generality of Time-Resolved Anisotropy for FRET Analysis using Ionic Strength Sensors as Model Systems

Previously, Currie *et al*.[52] and Leopold *et al*.[51] used time-resolved anisotropy of macromolecular crowding sensors as model systems as a proof of principle. In this approach, the fluorescence depolarization of donor-linker-acceptor constructs was attributed to both rotational dynamics and the energy transfer from the donor to the acceptor and was used for FRET analysis in response to crowding. Using the time-resolved fluorescence of the ionic strength sensors as a benchmark or a point of reference, Aplin *et al*. examined whether time-resolved anisotropy (Figure 3) can be generalized and used for quantifying the FRET efficiency and donor-acceptor distance of RD, RE, and KE in response to the environmental ionic strength of the Hofmeister salts such as Na_2SO_4, NaI, NaCl, and KCl.[57]

The time-resolved fluorescence depolarization of intact ionic strength sensors decayed as a biexponential at rates depending on the energy transfer rate (fast component) and the overall rotational dynamics (slow component) (Equation 7, Figure 3). In this model, the ensemble population was assumed to consist of a FRETing subpopulation and another that is non-FRETing due to unfavorable conformation or orientation parameters. In contrast, the time-resolved fluorescence depolarization of the cleaved sensors decayed as a single exponential with a rotational time that is consistent with the size of the donor alone (mCerulean3). FRET-capable intact sensors and FRET-incapable cleaved sensors were distinct and sensitive to salt concentration. In agreement with Miller *et al*., Aplin and colleagues reported that the FRET efficiency of the ionic strength sensors decreased as the ionic strength (e.g., KCl concentration) increased, which was due to the increased donor-acceptor distance at higher salt concentrations.[55,57]

Aplin *et al*. also reported a slight difference in the sensitivity of the KE sensor to the type of salt or dissolved ions.[57] For example, they observed that the largest response was observed at the Na_2SO_4 concentration below 150 mM and reached a plateau above 150 mM of the same salt, which is distinct from the response to NaI and NaCl concentrations. The plateau in response to Na_2SO_4 is then hypothesized to be the result of an increased number of charges in solution potentially resulting in saturation of the linker region preventing significant changes in intramolecular linker interactions. While both NaI and NaCl produce the same ionic strength in solution, KE displayed a larger response to NaI than NaCl, which was attributed to potential sensitivity to the anion identity. They proposed that the iodide ion might be less hydrated than chlorine in solution and therefore has more interactions with the charged linker region of KE.[57]

Using the time-resolved depolarization of these ionic strength sensors, Aplin *et al*. also offered a thermodynamic analysis of the equilibrium kinetics associated with the conformational changes of these sensors in response to the environmental ionic strength.[57] Using the amplitude fractions of the FRETing (collapsed structure) and non-FRETing (stretched structure) subpopulations, Aplin *et al*. reported approximate values of both the associated equilibrium constant (K) and Gibbs free energy (ΔG) of KE as a function of KCl concentrations. The results suggested that stretched conformation of these sensors was favored at higher ionic strength (e.g., higher KCl concentrations), a conclusion that agrees with the observed reduction of the FRET efficiency and enhanced donor-acceptor distance at higher ionic strength. Taken together, these results support the hypothesis that as the ionic strength increases, the dissolved ions will reduce the electrostatic interaction (Debye ionic shielding) between the two oppositely charged α-helices in the linker region and therefore will increase the donor-acceptor distance, which leads to a reduction in the FRET efficiency in a manner that is sensitive to the type of dissolved ions.[55,57]

4. CONCLUSIONS AND FUTURE DIRECTIONS

In this mini-review, we highlighted recent advances in genetically encoded sensors for both environmental ionic strength and macromolecular crowding in controlled solutions. These studies examined different molecular engineering aspects (e.g., length, flexibility, and charges in the linker region) towards the development of rational design strategies for highly sensitive environmental sensors for a wide range of *in vivo* applications. In addition, these donor-linker-acceptor constructs were used as model molecular systems for developing new noninvasive, quantitative methods for FRET analysis in response to changes in the surrounding environments. For example, the standard time–resolved fluorescence of the donor in the presence and absence of the acceptor was used for FRET analysis in these sensors. Using these measurements as a point of reference, other techniques were also developed for FRET analysis such as time-resolved depolarization where the donor is excited and the polarization analysis of the predominantly acceptor's emission was used to determining the energy transfer rate. At the single molecule level, the molecular brightness of the donor in the presence and absence of the acceptor were also measured using FCS for FRET analysis and compared with the ensemble studies.

Taken together, these studies of donor-linker-acceptor sensors in controlled solutions showed a great potential for future *in vivo* applications, which would also benefit from the laser-induced fluorescence methodologies developed that are also compatible with *in vivo* imaging for mapping cellular microenvironments under different physiological and pathological conditions. From the molecular design perspective, sensors with donor-acceptor FRET pairs, where the donor can be excited using laser wavelengths commonly accessible to research laboratories, or where the FRET pair is red-shifted to decrease the background signal of a cell. Recently, for example, Boersma and coworkers have developed GE2.3 (mEGFP-linker-mScarlet–I) that can be excited at 488-nm.[68,69] In addition, Miyagi *et al*. have developed a genetically encoded macromolecular crowding sensor (CRONOS) that consists of mNeonGreen-linker-mScarlet–I, where the donor can also be excited at 506-nm.[70] It was reported that CRONOS is bright biosensor with a large dynamic range that suited for live cell studies with various modalities. Genetically-encoded, intrinsically fluorescent protein-based sensors, combined with quantitative non-invasive fluorescence spectroscopy methods, have a great potential for site-specific mapping of heterogeneous microenvironments in living cells for macromolecular crowding or ionic strength sensing.

ACKNOWLEDGEMENTS

We would like to thank Sarah Bergman for her help in the laboratory and data analysis. We also acknowledge the financial support and teaching assistantships (S.A.M., R.S., and M.J.B.) of the Department of Chemistry and Biochemistry, Swenson College of Science and Engineering, University of Minnesota Duluth. E.D.S. and

A.A.H also acknowledge the support of the University of Minnesota Grant-in-Aid, University of Minnesota Duluth Chancellor's Small Grant, and Minnesota Supercomputing Institute (MSI) at the University of Minnesota.

REFERENCES

[1] Datta, R., Heaster, T. M., Sharick, J. T., Gillette, A. A. and Skala, M. C., "Fluorescence lifetime imaging microscopy: fundamentals and advances in instrumentation, analysis, and applications," J. Biomed. Opt. **25**(07), 1 (2020).

[2] Yang, G., Liu, Y., Teng, J. and Zhao, C.-X., "FRET Ratiometric Nanoprobes for Nanoparticle Monitoring," Biosensors **11**(12), 505 (2021).

[3] Ranawat, H., Pal, S. and Mazumder, N., "Recent trends in two-photon auto-fluorescence lifetime imaging (2P-FLIM) and its biomedical applications," Biomed. Eng. Lett. **9**(3), 293–310 (2019).

[4] Liu, X., Lin, D., Becker, W., Niu, J., Yu, B., Liu, L. and Qu, J., "Fast fluorescence lifetime imaging techniques: A review on challenge and development," J. Innov. Opt. Health Sci. **12**(05), 1930003 (2019).

[5] Pastore, A. and Temussi, P. A., "Crowding revisited: Open questions and future perspectives," Trends Biochem. Sci., S0968000422001402 (2022).

[6] Konopka, M. C., Shkel, I. A., Cayley, S., Record, M. T. and Weisshaar, J. C., "Crowding and Confinement Effects on Protein Diffusion In Vivo," J. Bacteriol. **188**(17), 6115–6123 (2006).

[7] Zhou, H.-X., Rivas, G. and Minton, A. P., "Macromolecular Crowding and Confinement: Biochemical, Biophysical, and Potential Physiological Consequences," Annu. Rev. Biophys. **37**(1), 375–397 (2008).

[8] Gnutt, D. and Ebbinghaus, S., "The macromolecular crowding effect – from in vitro into the cell," Biol. Chem. **397**(1), 37–44 (2016).

[9] Minton, A. P., "The Influence of Macromolecular Crowding and Macromolecular Confinement on Biochemical Reactions in Physiological Media," J. Biol. Chem. **276**(14), 10577–10580 (2001).

[10] Mourão, M. A., Hakim, J. B. and Schnell, S., "Connecting the Dots: The Effects of Macromolecular Crowding on Cell Physiology," Biophys. J. **107**(12), 2761–2766 (2014).

[11] Minton, A. P. and Wilf, J., "Effect of macromolecular crowding upon the structure and function of an enzyme: glyceraldehyde-3-phosphate dehydrogenase," Biochemistry **20**(17), 4821–4826 (1981).

[12] Zimmerman, S. B. and Trach, S. O., "Estimation of macromolecule concentrations and excluded volume effects for the cytoplasm of Escherichia coli," J. Mol. Biol. **222**(3), 599–620 (1991).

[13] Hall, D. and Minton, A. P., "Macromolecular crowding: qualitative and semiquantitative successes, quantitative challenges," Biochim. Biophys. Acta BBA - Proteins Proteomics **1649**(2), 127–139 (2003).

[14] Murade, C. U. and Shubeita, G. T., "A Molecular Sensor Reveals Differences in Macromolecular Crowding between the Cytoplasm and Nucleoplasm," ACS Sens. **4**(7), 1835–1843 (2019).

[15] Salis, A., Bilaničová, D., Ninham, B. W. and Monduzzi, M., "Hofmeister Effects in Enzymatic Activity: Weak and Strong Electrolyte Influences on the Activity of *Candida rugosa* Lipase," J. Phys. Chem. B **111**(5), 1149–1156 (2007).

[16] Spitzer, J. and Poolman, B., "The Role of Biomacromolecular Crowding, Ionic Strength, and Physicochemical Gradients in the Complexities of Life's Emergence," Microbiol. Mol. Biol. Rev. **73**(2), 371–388 (2009).

[17] Mitchison, T. J., "Colloid osmotic parameterization and measurement of subcellular crowding," Mol. Biol. Cell **30**(2), D. Kellogg, Ed., 173–180 (2019).

[18] Gnutt, D., Gao, M., Brylski, O., Heyden, M. and Ebbinghaus, S., "Excluded-Volume Effects in Living Cells," Angew. Chem. Int. Ed. **54**(8), 2548–2551 (2015).

[19] Tokuriki, N., "Protein folding by the effects of macromolecular crowding," Protein Sci. **13**(1), 125–133 (2004).

[20] Cuevas-Velazquez, C. L., Vellosillo, T., Guadalupe, K., Schmidt, H. B., Yu, F., Moses, D., Brophy, J. A. N., Cosio-Acosta, D., Das, A., Wang, L., Jones, A. M., Covarrubias, A. A., Sukenik, S. and Dinneny, J. R., "Intrinsically disordered protein biosensor tracks the physical-chemical effects of osmotic stress on cells," Nat. Commun. **12**(1), 5438 (2021).

[21] König, I., Soranno, A., Nettels, D. and Schuler, B., "Impact of In□Cell and In□Vitro Crowding on the Conformations and Dynamics of an Intrinsically Disordered Protein," Angew. Chem. **133**(19), 10819–10824 (2021).

[22] Weiss, M., "Crowding, Diffusion, and Biochemical Reactions," [International Review of Cell and Molecular Biology], Elsevier, 383–417 (2014).

[23] Kim, S. A., Heinze, K. G. and Schwille, P., "Fluorescence correlation spectroscopy in living cells," Nat. Methods **4**(11), 963–973 (2007).

[24] Hess, S. T., Huang, S., Heikal, A. A. and Webb, W. W., "Biological and Chemical Applications of Fluorescence Correlation Spectroscopy: A Review," Biochemistry **41**(3), 697–705 (2002).

[25] Elson, E. L., "Fluorescence Correlation Spectroscopy: Past, Present, Future," Biophys. J. **101**(12), 2855–2870 (2011).

[26] Manzo, C. and Garcia-Parajo, M. F., "A review of progress in single particle tracking: from methods to biophysical insights," Rep. Prog. Phys. **78**(12), 124601 (2015).

[27] Junker, N. O., Vaghefikia, F., Albarghash, A., Höfig, H., Kempe, D., Walter, J., Otten, J., Pohl, M., Katranidis, A., Wiegand, S. and Fitter, J., "Impact of Molecular Crowding on Translational Mobility and Conformational Properties of Biological Macromolecules," J. Phys. Chem. B **123**(21), 4477–4486 (2019).

[28] Delarue, M., Brittingham, G. P., Pfeffer, S., Surovtsev, I. V., Pinglay, S., Kennedy, K. J., Schaffer, M., Gutierrez, J. I., Sang, D., Poterewicz, G., Chung, J. K., Plitzko, J. M., Groves, J. T., Jacobs-Wagner, C., Engel, B. D. and Holt, L. J., "mTORC1 Controls Phase Separation and the Biophysical Properties of the Cytoplasm by Tuning Crowding," Cell **174**(2), 338-349.e20 (2018).

[29] Li, H., Dou, S.-X., Liu, Y.-R., Li, W., Xie, P., Wang, W.-C. and Wang, P.-Y., "Mapping Intracellular Diffusion Distribution Using Single Quantum Dot Tracking: Compartmentalized Diffusion Defined by Endoplasmic Reticulum," J. Am. Chem. Soc. **137**(1), 436–444 (2015).

[30] Pierobon, P. and Cappello, G., "Quantum dots to tail single bio-molecules inside living cells," Adv. Drug Deliv. Rev. **64**(2), 167–178 (2012).

[31] Hämisch, B., Pollak, R., Ebbinghaus, S. and Huber, K., "Self□Assembly of Pseudo□Isocyanine Chloride as a Sensor for Macromolecular Crowding In Vitro and In Vivo," Chem. – Eur. J. **26**(31), 7041–7050 (2020).

[32] Kaur, B., Kaur, N. and Kumar, S., "Colorimetric metal ion sensors – A comprehensive review of the years 2011–2016," Coord. Chem. Rev. **358**, 13–69 (2018).

[33] Biemans-Oldehinkel, E., Mahmood, N. A. B. N. and Poolman, B., "A sensor for intracellular ionic strength," Proc. Natl. Acad. Sci. **103**(28), 10624–10629 (2006).

[34] Moussa, R., Baierl, A., Steffen, V., Kubitzki, T., Wiechert, W. and Pohl, M., "An evaluation of genetically encoded FRET-based biosensors for quantitative metabolite analyses in vivo," J. Biotechnol. **191**, 250–259 (2014).

[35] Wolfbeis, O. S. and Offenbacher, H., "Fluorescence sensor for monitoring ionic strength and physiological pH values," Sens. Actuators **9**(1), 85–91 (1986).

[36] Altamash, T., Ahmed, W., Rasool, S. and Biswas, K. H., "Intracellular Ionic Strength Sensing Using NanoLuc," Int. J. Mol. Sci. **22**(2), 677 (2021).

[37] Sarder, P., Maji, D. and Achilefu, S., "Molecular Probes for Fluorescence Lifetime Imaging," Bioconjug. Chem. **26**(6), 963–974 (2015).

[38] Clegg, R. M., "Chapter 1 Förster resonance energy transfer—FRET what is it, why do it, and how it's done," [Laboratory Techniques in Biochemistry and Molecular Biology], Elsevier, 1–57 (2009).

[39] Piston, D. W. and Kremers, G.-J., "Fluorescent protein FRET: the good, the bad and the ugly," Trends Biochem. Sci. **32**(9), 407–414 (2007).

[40] Lakowicz, J. R., [Principles of fluorescence spectroscopy, 3rd ed], Springer, New York (2006).

[41] Förster, T., "Energy migration and fluorescence," J. Biomed. Opt. **17**(1), 011002 (2012).

[42] Zeug, A., Woehler, A., Neher, E. and Ponimaskin, E. G., "Quantitative Intensity-Based FRET Approaches—A Comparative Snapshot," Biophys. J. **103**(9), 1821–1827 (2012).

[43] Padilla-Parra, S. and Tramier, M., "FRET microscopy in the living cell: Different approaches, strengths and weaknesses," BioEssays **34**(5), 369–376 (2012).

[44] Lerner, E., Cordes, T., Ingargiola, A., Alhadid, Y., Chung, S., Michalet, X. and Weiss, S., "Toward dynamic structural biology: Two decades of single-molecule Förster resonance energy transfer," Science **359**(6373), eaan1133 (2018).

[45] Lerner, E., Barth, A., Hendrix, J., Ambrose, B., Birkedal, V., Blanchard, S. C., Börner, R., Sung Chung, H., Cordes, T., Craggs, T. D., Deniz, A. A., Diao, J., Fei, J., Gonzalez, R. L., Gopich, I. V., Ha, T., Hanke, C. A., Haran, G., Hatzakis, N. S., et al., "FRET-based dynamic structural biology: Challenges, perspectives and an appeal for open-science practices," eLife **10**, e60416 (2021).

[46] Boersma, A. J., Zuhorn, I. S. and Poolman, B., "A sensor for quantification of macromolecular crowding in living cells," Nat. Methods **12**(3), 227–229 (2015).

[47] Liu, B., Mavrova, S. N., van den Berg, J., Kristensen, S. K., Mantovanelli, L., Veenhoff, L. M., Poolman, B. and Boersma, A. J., "Influence of Fluorescent Protein Maturation on FRET Measurements in Living Cells," ACS Sens. **3**(9), 1735–1742 (2018).

[48] Markwardt, M. L., Kremers, G.-J., Kraft, C. A., Ray, K., Cranfill, P. J. C., Wilson, K. A., Day, R. N., Wachter, R. M., Davidson, M. W. and Rizzo, M. A., "An Improved Cerulean Fluorescent Protein with Enhanced Brightness and Reduced Reversible Photoswitching," PLoS ONE **6**(3), D. Jones, Ed., e17896 (2011).

[49] Liu, B., Åberg, C., van Eerden, F. J., Marrink, S. J., Poolman, B. and Boersma, A. J., "Design and Properties of Genetically Encoded Probes for Sensing Macromolecular Crowding," Biophys. J. **112**(9), 1929–1939 (2017).

[50] Schwarz, J., J Leopold, H., Leighton, R., Miller, R. C., Aplin, C. P., Boersma, A. J., Heikal, A. A. and Sheets, E. D., "Macromolecular crowding effects on energy transfer efficiency and donor-acceptor distance of hetero-FRET sensors using time-resolved fluorescence," Methods Appl. Fluoresc. **7**(2), 025002 (2019).

[51] Leopold, H. J., Leighton, R., Schwarz, J., Boersma, A. J., Sheets, E. D. and Heikal, A. A., "Crowding Effects on Energy-Transfer Efficiencies of Hetero-FRET Probes As Measured Using Time-Resolved Fluorescence Anisotropy," J. Phys. Chem. B **123**(2), 379–393 (2019).

[52] Currie, M., Leopold, H., Schwarz, J., Boersma, A. J., Sheets, E. D. and Heikal, A. A., "Fluorescence Dynamics of a FRET Probe Designed for Crowding Studies," J. Phys. Chem. B **121**(23), 5688–5698 (2017).

[53] Kay, T. M., Aplin, C. P., Simonet, R., Beenken, J., Miller, R. C., Libal, C., Boersma, A. J., Sheets, E. D. and Heikal, A. A., "Molecular Brightness Approach for FRET Analysis of Donor-Linker-Acceptor Constructs at the Single Molecule Level: A Concept," Front. Mol. Biosci. **8**, 730394 (2021).

[54] Pittas, T., Zuo, W. and Boersma, A. J., "Engineering crowding sensitivity into protein linkers," [Methods in Enzymology], Elsevier, 51–81 (2021).

[55] Miller, R. C., Aplin, C. P., Kay, T. M., Leighton, R., Libal, C., Simonet, R., Cembran, A., Heikal, A. A., Boersma, A. J. and Sheets, E. D., "FRET Analysis of Ionic Strength Sensors in the Hofmeister Series of Salt Solutions Using Fluorescence Lifetime Measurements," J. Phys. Chem. B **124**(17), 3447–3458 (2020).

[56] Fisz, J. J., "Another Look at Magic-Angle-Detected Fluorescence and Emission Anisotropy Decays in Fluorescence Microscopy," J. Phys. Chem. A **111**(50), 12867–12870 (2007).

[57] Aplin, C. P., Miller, R. C., Kay, T. M., Heikal, A. A., Boersma, A. J. and Sheets, E. D., "Fluorescence depolarization dynamics of ionic strength sensors using time-resolved anisotropy," Biophys. J. **120**(8), 1417–1430 (2021).

[58] Shashkova, S. and Leake, M. C., "Single-molecule fluorescence microscopy review: shedding new light on old problems," Biosci. Rep. **37**(4), BSR20170031 (2017).

[59] Moerner, W. E. and Fromm, D. P., "Methods of single-molecule fluorescence spectroscopy and microscopy," Rev. Sci. Instrum. **74**(8), 3597–3619 (2003).

[60] Yu, L., Lei, Y., Ma, Y., Liu, M., Zheng, J., Dan, D. and Gao, P., "A Comprehensive Review of Fluorescence Correlation Spectroscopy," Front. Phys. **9**, 644450 (2021).

[61] Tian, Y., Martinez, M. M. and Pappas, D., "Fluorescence Correlation Spectroscopy: A Review of Biochemical and Microfluidic Applications," Appl. Spectrosc. **65**(4), 115–124 (2011).

[62] Haupts, U., Maiti, S., Schwille, P. and Webb, W. W., "Dynamics of fluorescence fluctuations in green fluorescent protein observed by fluorescence correlation spectroscopy," Proc. Natl. Acad. Sci. **95**(23), 13573–13578 (1998).

[63] Sreenivasan, V. K. A., Graus, M. S., Pillai, R. R., Yang, Z., Goyette, J. and Gaus, K., "Influence of FRET and fluorescent protein maturation on the quantification of binding affinity with dual-channel fluorescence cross-correlation spectroscopy," Biomed. Opt. Express **11**(11), 6137 (2020).

[64] Price, E. S., DeVore, M. S. and Johnson, C. K., "Detecting Intramolecular Dynamics and Multiple Förster Resonance Energy Transfer States by Fluorescence Correlation Spectroscopy," J. Phys. Chem. B **114**(17), 5895–5902 (2010).

[65] Chen, A., Eberle, M. M., Lunt, E. J., Liu, S., Leake, K., Rudenko, M. I., Hawkins, A. R. and Schmidt, H., "Dual-color fluorescence cross-correlation spectroscopy on a planar optofluidic chip," Lab. Chip **11**(8), 1502 (2011).

[66] Schwille, P., Meyer-Almes, F. J. and Rigler, R., "Dual-color fluorescence cross-correlation spectroscopy for multicomponent diffusional analysis in solution," Biophys. J. **72**(4), 1878–1886 (1997).

[67] Liu, B., Poolman, B. and Boersma, A. J., "Ionic Strength Sensing in Living Cells," ACS Chem. Biol. **12**(10), 2510–2514 (2017).

[68] Mouton, S. N., Thaller, D. J., Crane, M. M., Rempel, I. L., Terpstra, O. T., Steen, A., Kaeberlein, M., Lusk, C. P., Boersma, A. J. and Veenhoff, L. M., "A physicochemical perspective of aging from single-cell analysis of pH, macromolecular and organellar crowding in yeast," eLife **9**, e54707 (2020).

[69] Guerzoni, L. P. B., de Goes, A. V. C., Kalacheva, M., Haduła, J., Mork, M., De Laporte, L. and Boersma, A. J., "High Macromolecular Crowding in Liposomes from Microfluidics," Adv. Sci., 2201169 (2022).

[70] Miyagi, T., Yamanaka, Y., Harada, Y., Narumi, S., Hayamizu, Y., Kuroda, M. and Kanekura, K., "An improved macromolecular crowding sensor CRONOS for detection of crowding changes in membrane-less organelles under stressed conditions," Biochem. Biophys. Res. Commun. **583**, 29–34 (2021).